Asia-Pacific Journal of Atmospheric Sciences (2020) 56:321–331
https://doi.org/10.1007/s13143-019-00124-x

Online ISSN 1976-7951
Print ISSN 1976-7633

ORIGINAL ARTICLE

Decoding Tropospheric Ozone in Hangzhou, China: from Precursors to Sources

Rui Feng[1,2,3,4] · Kun Luo[1] · Jian-ren Fan[1]

Received: 4 September 2018 / Revised: 10 April 2019 / Accepted: 19 April 2019 / Published online: 17 May 2019

Abstract

For the purpose of providing a tropospheric O_3 control strategy for Hangzhou, China, we investigate the influential factors of it using observed data and the WRF-CMAQ model. The result indicates that temperature and relative humidity are the dominant factors and Hangzhou belongs to VOC-limited regime. Long-range/regional transport accounts for 15.4% and 17.4% of O_3 in autumn and winter, respectively, showing a north-to-south transport pattern while 14.5% and 19.7% of O_3 in spring and summer, respectively, showing a southwest-to-northeast transport pattern. Annual contribution of local industry to local O_3 was 59.2%, followed by residence, traffic and agriculture. Ethylene, m/p-xylene, toluene and propylene are the main O_3 producers. Therefore, controlling VOCs species that possess the highest ozone formation potentials, afforestation, implementing artificial precipitation and shutdown local industry are the most effective ways to mitigate ozone pollution in Hangzhou.

Keywords O_3-VOC-NOx · Ozone formation potentials · WRF-CMAQ · Regional/long-range transport · Local sector contribution

1 Introduction

Tropospheric ozone (ground-level O_3) has negative influence on air quality and ecosystem (Telesnicki et al. 2018; Tai and Martin 2016; Marais et al. 2014). It has become the primary pollutant in China during recent summertime (Chan and Yao 2008; Liu et al. 2018a), thus causing accelerated climate change, increased mortality, elevated morbidity, escalated fiscal spending, declined economy vitality and recession on crops yield (Tambo et al. 2016; Zhang et al. 2018; Song et al. 2017; Hua et al. 2018; Wu et al. 2018; Zhang et al. 2014). The Yangtze River Delta (YRD), one of the most prosperous regions in China, suffered from severe O_3 pollution over the past decade (Liao et al. 2016; Li et al. 2018a; Fu et al. 2017, Chen et al. 2018; Feng et al. 2019). Hangzhou, the host of the G20 summit in 2016, the FINA short course world championships in 2018 and the Asian Games in 2022, is the second largest city in the YRD with population over nine million. The annual average concentration of ground-level O_3-8h (average of highest concentration of eight consecutive hours in a day) was 167 $\mu g/m^3$ in the summer of 2016, thus becoming the primary atmospheric pollutant since then. Therefore, it's of importance to make proper O_3 regulations for the good of local citizens and incoming Asian Games.

O_3 is strongly connected to its precursors and meteorological conditions, non-linearly depending on the concentration of HONO, NOx ($NO+NO_2$) and volatile organic compounds (VOCs) with the presence of solar radiation (Chan et al. 2017; Gao et al. 2016, 2017). High temperature, low relative humidity and low wind velocity lead to O_3 episodes (Li et al. 2017). As for the regional transport, the accumulation of ground-level O_3 over eastern China is dominated by photochemistry

Responsible Editor: Yunsoo Choi.

✉ Rui Feng
11727081@zju.edu.cn

✉ Kun Luo
zjulk@zju.edu.cn

[1] State Key Laboratory of Clean Energy Utilization, Zhejiang University, Hangzhou 310027, People's Republic of China

[2] China National Building Materials Group Corporation, China New Building Materials Design and Research Institute, Hangzhou 310022, People's Republic of China

[3] Department of chemical and biological engineering, University of Sheffield, Sheffield S10 2TN, UK

[4] College of biological sciences, University of Minnesota-Twin cities, Minneapolis, MN 55455, USA

and vertical transport in summer while by horizontal advection in spring, autumn and winter (Liu et al. 2010). From Ito et al. (2018), O_3 consums NOx to form particulate matter in dry weather. Urban heat island (UHI) and O_3 pollution over the YRD are positively correlated (Wang et al. 2018a). Wie and Moon (2018) suggest that enhanced Western North Pacific Subtropical High leads to an increasing in ground-level O_3 in South Korea. From Oyola et al. (2017), weather is the main driven force of O_3 variability. Alvim et al. (2017) point out that reducing the oxygenated VOCs is the most effective solution to limit O_3.

This study focuses on investigating the ozone formation processes, long range transport and local sector contributions in Hangzhou using the observed data from July 2016 to December 2017 and the Weather Research and Forecasting coupled with Community Multi-scale Air Quality (WRF-CMAQ) model to propose a feasible ground-level O_3 control strategy.

2 Methodology

2.1 Observation

We sampled and recorded the hourly atmospheric pollutants data from two local environmental monitoring stations: (a) Transferred Pond Environmental Monitoring Station (30.193 °N, 120.070 °E) locates at the Westlake National Park, representing scenic spot of Hangzhou; (b) Leaching Melon Environmental Monitoring Station (30.187 °N, 120.459 °E) locates near Hangzhou International Airport, representing rural Hangzhou. The hourly meteorological data were measured at the Transferred Pond Environmental Monitoring Station. Gas chromatography coupled with mass spectrometer (GC/MS) was used to measure 55 VOCs species, including alkanes, alkenes, alkynes and aromatics.

2.2 Simulation

The WRF-CMAQ model, also called the third generation of air quality simulation system, consists of three parts: pollution inventory, the meteorological model and the air quality model. The simulation process includes three steps. Firstly, WRF, a meso-scale weather forecast model, provided simulated meteorological data, such as atmospheric pressure, temperature, relative humidity, wind speed and wind direction. Secondly, pollution inventory pinpointed the anthropogenic and biogenic air pollution emission sources. Thirdly, the simulated meteorological data and gridded pollution sources generated from the first two steps were input in CMAQ to simulate the concentrations of O_3 in Hangzhou.

2.2.1 WRF Configuration

We used WRF version 3.4 for this study. The topographical data were derived from the WRF input data-set. The analytical data of troposphere were derived from the National Centers for Environmental Prediction (NCEP) (http://dss.ucar.edu/datasets/ds083.2/) in every 6 hours on 1° × 1° resolution. The main options for WRF are listed in Table 1.

2.2.2 Anthropogenic and Biogenic Pollution Inventory

The biogenic emissions of gases and aerosols from terrestrial ecosystems into the atmosphere were conducted by the Model of Emissions of Gases and Aerosols from Nature (MEGAN) version 2.04 (Wang et al. 2017). MEGAN required WRF-simulated meteorology and land cover data to drive. Land cover data is divided into Leaf Area Index (LAI), Plant Function Type (PFT) and Emission Factor (ET). LAI (total area of leaves divided by land area), whose global spatial resolution was 30s, was extracted from Moderate Resolution Imaging Spectroradiometer (MODIS) (Barnes et al. 2019) database from National Aeronautics and Space Administration (NASA); PFT, including broad-leaves, conifer, herb (crops and grass) and shrub, was derived from the MODIS and the forest census by China Bureau of Forest Resource.

The anthropogenic inventory of China (http://www.meicmodel.org/) was created by Tsinghua University in 0.5 ° × 0.5 ° in 2016, including all common atmospheric pollutants, such as SO_2, NOx, CO, $PM_{2.5}$, PM_{10} and VOCs (Zhao et al. 2018). Shanghai Academy of Environmental Sciences upgraded the anthropogenic inventory upon YRD (Liu et al. 2018b; Feng et al. 2018).

2.2.3 CMAQ Model

The CMAQ had five modules. Initial Conditions Processor provided initial field. Boundary Conditions Processor provided boundary. Photolysis Rate Processor gave the photolysis rate. Meteorology-Chemistry Interface Processor transformed

Table 1 Main options for WRF

Parameter	Selected scheme
Microphysical process	WSM6 (Xiao et al. 2013)
Long wave radiation	RRTM (Fountoukis et al. 2018)
Short wave radiation	Goddard (Mohr et al. 2013)
Ground-level surface layer	Monin-Obukhov (Breedt et al. 2018)
Land surface process	Noah (Kishné et al. 2017)
Boundary layer	YSU (Dong et al. 2018)
Cumulus parameterization	Grell-Devenyi (Zepka et al. 2014)

the WRF-simulated meteorology into the data format required by CMAQ. CMAQ Chemistry-Transport Model (CCTM), the core of CMAQ, was a mathematical model for atmospheric physics and chemistry.

The CMAQ version 5.0.2 was used for this study using the Lambert projection coordinate. Three nested domains were used for simulation. The first domain covered entire China and the grid number was 173 × 136 in 36 km resolution. The second domain covered eastern China and grid number was 135 × 228 in 12 km resolution. The third domain covered the YRD and the grid number was 150 × 174 in 4 km resolution. The vertical direction was divided into 14 layers with denser layers near the ground. The top was set at 100 hpa. CB05 and AERO6 were chosen for the gas-phase chemical reaction mechanism and aerosol mechanism, respectively.

3 Results and Discussions

3.1 Observation based analysis

3.1.1 Influential Factors Analysis

O_3-8h was set as the highest average of the measured ozone from eight consecutive hours in a day. Since most of VOCs emission industries in Hangzhou had been shut down from late July to mid-September in 2016 by strict administrative control because of the policy that intended to improve the air quality during G20 summit, the VOCs of scenic spot was much lower than that of the rural area. According to Fig. 1, the yearly trends of ground-level O_3 with NO_2 in the scenic spot of Hangzhou and rural Hangzhou both were negative correlated. O_3 was most abundant in summer and lowest in winter while NO_2 was on the contrary. The monthly ratio of NO_2 to non-methane total hydrocarbons (NMHC) ranged from 0.89 to 2.47 with average 1.74. According to the empirical kinetic modeling approach (EKMA) (Tan et al. 2018), Hangzhou belongs to VOC-limited regime. Reduction of NOx or escalation of VOCs resulted in elevation of ground-level O_3 and vice versa (Feng et al. 2018). Shanghai, the largest city in YRD, also belongs to VOC-limited regime (Geng et al. 2009; Tie et al. 2013; Gao et al. 2017), as Hangzhou and Shanghai have the similar meteorological conditions, air pollution emission sources and energy structures (Geng et al. 2011; Tie et al. 2013; Geng et al. 2008; Qian 2015; Wu 1999; Xu et al. 2017). The average O_3-8h, NO_2 and VOCs at scenic spot were 150.4 μg/m^3, 31.4 μg/m^3 and 7.9 ppbv, respectively, while the average O_3-8h, NOx and VOCs in rural areas were 163.2 μg/m^3, 30.9 μg/m^3 and 19.5 ppbv, respectively, in August 2016. VOCs increased by 146.8%, NO_2 remained steady, and O_3 increased by 12.8 μg/m^3, demonstrating Hangzhou is VOC-limited. The average O_3-8h, NO_2 and VOCs at scenic spot were 126.4 μg/m^3, 57.7 μg/m^3 and 23.8 ppbv, respectively, while the average O_3-8h, NOx and VOCs in rural areas were 141.0 μg/m^3, 30.3 μg/m^3 and 22.9 ppbv, respectively, in August 2017, indicating Hangzhou is VOC-limited as well.

From Fig. 1, the meteorology of Hangzhou inferred O_3 were positively correlated to temperature and direct solar irradiation time while negatively correlated to precipitation and relative humidity. The steady wind speed ranging from 2.0 m/s to 2.8 m/s suggested the stable monthly regional transport O_3 by advection. The Asia-Pacific monsoon, greatly affects seasonal ground-level O_3 in East Asian through impacting on temperature, direct solar radiation time, precipitation and relative humidity (Li et al. 2018b; Hou et al. 2015). The Asia-Pacific monsoon is dominated by the Western North Pacific Subtropical High (WNPSH) (Wie and Moon 2018). The most abundant rainfall and lowest direct solar radiation hours occurred in June 2017, so as the lowest level of O_3 from May to September of 2017 occurred in June, as Zhao and Wang (2017) prove that the lower ozone level over eastern China is influenced by moisture associated with WNPSH. Low relative humidity slows down the O_3 decomposition reaction rate (He et al. 2017). Lower relative humidity and longer solar radiation time facilitated ozone formation through photochemical reactions (Wang et al. 2009), accounting for the ozone episodes of Hangzhou in summer. Plus, according to the atmospheric pressure data derived from Hangzhou Bureau of meteorology, WNSPH usually influences Hangzhou from mid-May to mid-September in the last decades. Thus, in general, WNPSH is the dominant factor for meteorological conditions that influence ground-level O_3 in Hangzhou from mid-May to mid-September. Additionally, the ground-level O_3 in Hangzhou may also ascend due to the global warming effect (Li et al. 2018c).

Thus, we put forward an empirical formula to reveal the relationships among monthly average ground-level O_3-8h, its precursors and the meteorological conditions in Hangzhou:

$$C = \frac{ln(RH \times WS \times N \times O)}{ln(T \times V \times (S+2))} \quad (1)$$

Where RH is the relative humidity (%), WS is the wind speed (meter per second), N is the level of NO_2 (μg/m^3), O is the ground-level O_3 (μg/m^3), T is the temperature (Celsius), V is the level of VOCs (ppb) and S is the direct solar radiation time (hours). C ranges from 1.5 to 2.0 with average 1.75. We name C the ground-level ozone index (GOI) for Hangzhou. GOI implied the positive and negative correlated factors of ground-level O_3 in Hangzhou. GOI is also suitable to estimate the daily O_3-8h. Over 95% of GOI ranged from 1.7 to 2.3 with average 1.98 in wintertime and 1.3 to 1.7 with average 1.50 in summertime. As for spring and autumn, the outcome usually ranged between 1.5 and 1.9. This formula proves that O_3-

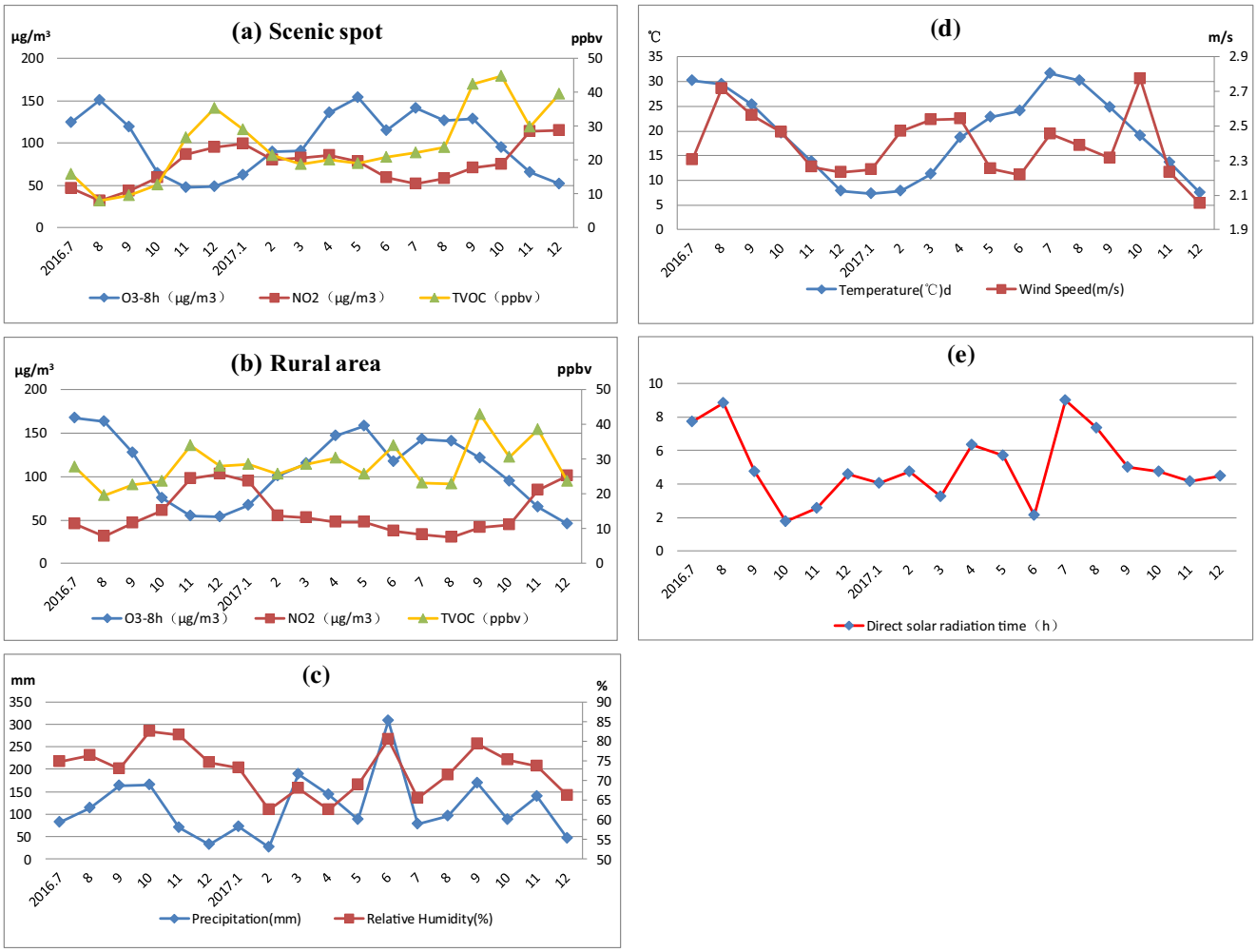

Fig. 1 The monthly average pollution and meteorological conditions of Hangzhou, **a** NO_2, VOCs and O_3 in scenic spot; **b** NO_2, VOCs and O_3 in rural areas; **c** precipitation and relative humidity; **d** temperature and wind speed; **e** direct solar radiation hours

8h is positively correlated with temperature, VOCs and direct solar radiation while negatively correlated with RH, wind speed and NO_2.

3.1.2 Wintertime and Summertime O_3 Analysis

The hourly data from January 11th to 18th and July 1st to 8th in 2017 at scenic spot were selected as the wintertime and summertime ozone investigation periods, respectively, because of the rapid fluctuation of O_3-8h, meteorology and precursors.

Wintertime From Fig. 2, the NO_2 and ground-level O_3 were negatively correlated in wintertime showing a strong VOC-limited pattern. When the NO_2 was over 60 μg/m^3, the ground-level O_3 concentration was less than 20 μg/m^3 during daytime. The hourly VOCs had great fluctuation but the daily average VOCs had the same the trend of daily O_3-8h. The diurnal (8:00 to 16:00) O_3 peaks of 13th, 14th, 15th and 16th follow the rules that the more the temperature raised and humidity reduced, the greater the amount of ground-level O_3 increased. The increased O_3 before the dawn of January 15th was mainly owing to the reduction of NO_2 during nighttime. Low temperature, high relative humidity and low direct solar radiation time were the main contributors of the steadily low O_3 period from 0 $_{AM}$ in 12th to 9 $_{AM}$ in 13th and 0 $_{AM}$ in 16th to 13 $_{PM}$ in 18th.

Summertime According to Fig. 3, the NO_2 and ground-level O_3 were also strongly negatively correlated in summer showing a strong VOC-limited pattern. The primary source of NO_2 is automobiles (Feng et al. 2019; Kumar et al. 2018; Zouzelka and Rathousky 2017), which is supposed to be higher during daytime. Thus, daytime O_3 was dominant in the NO_2-O_3 relationship to lower diurnal NO_2. Nighttime NO_2 restrained nocturnal O_3 level as NO_2 became the dominant without the solar radiation. Likewise wintertime, the low relative humidity and high temperature facilitated the formation of O_3. The

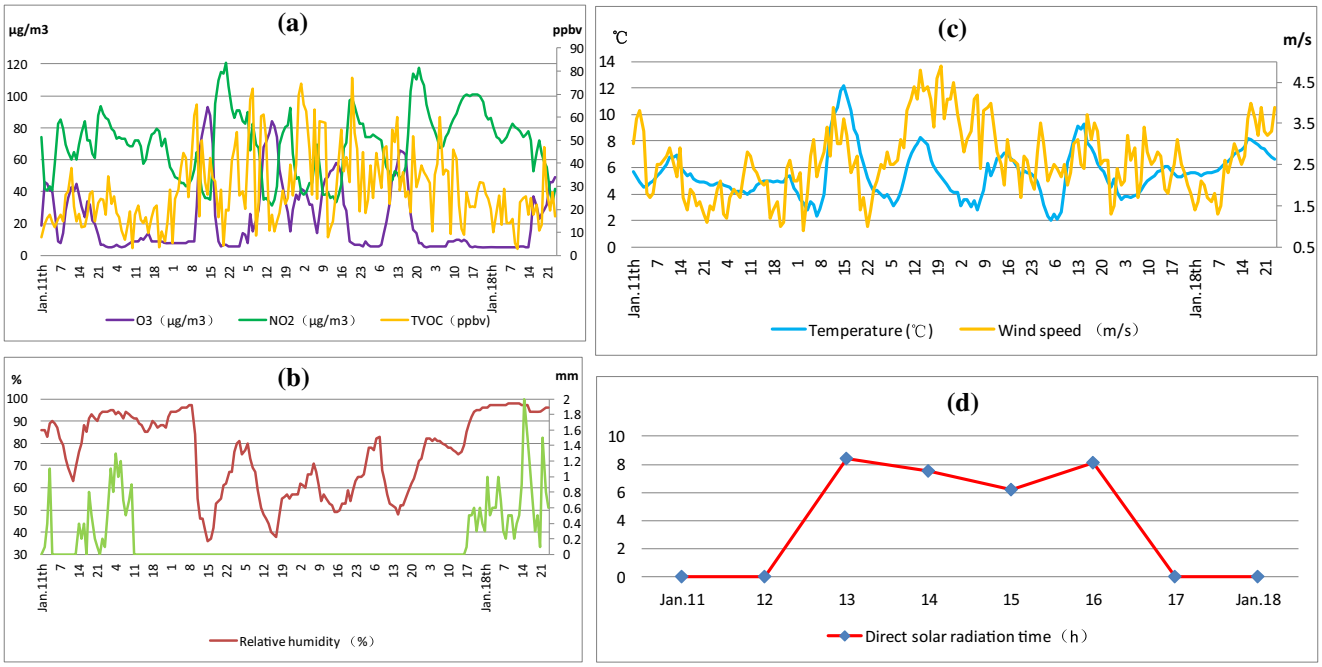

Fig. 2 January 11th to 18th in 2017 at scenic spot: **a** O_3, NO_2 and VOCs; **b** relative humidity and precipitation; **c** temperature and wind speed; **d** daily direct solar radiation hours

relatively low peak of O_3 on July 2nd was owing to the low direct solar radiation time. Lastly, when the daily direct solar radiation time was less than 4 h, it can greatly affect the O_3, but it became less effective in shaping O_3 when more than 4 h.

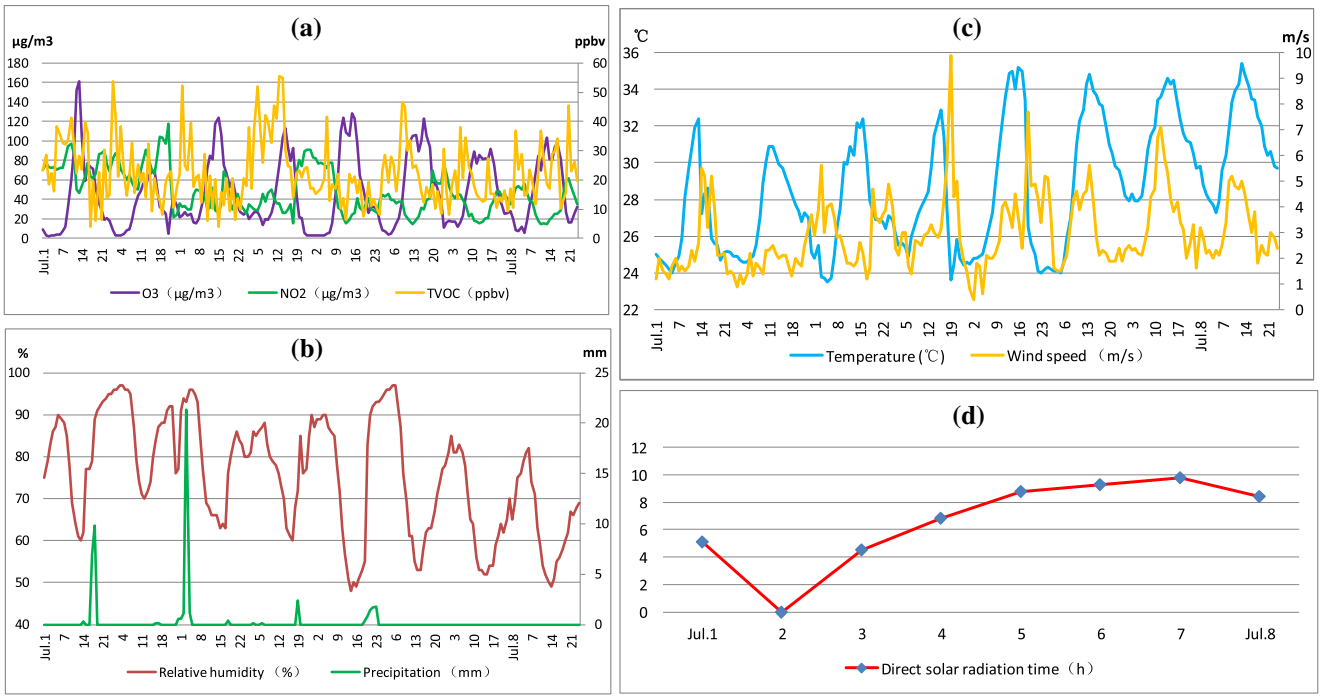

Fig. 3 July 1st to 8th in 2017 at scenic spot: **a** O_3, NO_2 and VOCs level; **b** relative humidity and precipitation; **c** temperature and wind speed; **d** daily direct solar radiation hours

3.1.3 VOCs Analysis

Due to the fact that Hangzhou government plans to reduce the annual NO_2 level to less than 40 μg/m^3 in the year of 2020, controlling the VOCs is one of the most effective ways to lower ground-level O_3. In the scenic spot, the annually average VOCs was 27.12 ppbv. Alkane, alkene, aromatics and acetylene accounted for 63.3%, 11.2%, 24.8% and 0.6%, respectively. In the rural area, the annually average VOCs were 29.51 ppbv. Alkane, alkene, aromatics and acetylene accounted for 65.6%, 8.3%, 24.8% and 1.3%, respectively. Ozone formation potential (OFP) (Carter 2010) is used for estimating how much O_3 can be produced by a single VOC species. The equation is shown below,

$$\mathrm{OFP} = \sum_i \mathrm{VOCi} \times \mathrm{MIR} \quad (2)$$

Where OFP is the ozone formation potential, VOC_i is the concentration of the VOC species i (g/m^3) and MIR is the maximum incremental reactivity (Wang et al. 2018b; Carter and Seinfeld 2012). The result indicated that alkane, alkene, aromatic and acetylene accounted for 22.1%, 43.6%, 34.2 and 0.1% of OFP in the scenic spot while 28.2%, 32.6%, 38.9%, 0.3% of OFP in the rural area, respectively. Although alkane was the most abundant subgroup of VOCs occupying more than 63% of total amount of emitted VOCs, the alkene and aromatic contributed more OFP in both scenic spot and rural areas due to maximum incremental reactivity, shown in Table 2. Therefore, controlling ethylene, m/p-xylene, toluene and propylene is the best way to mitigate the ground-level O_3 pollution in Hangzhou. Plus, the overall OFP of rural areas was 9.5% more than that of scenic spot in 2017. In addition, urban heat island (UHI) is also reported has impact on O_3 (Wang et al. 2018a; Li et al. 2016b; Ganeshan et al. 2013).

Table 2 Top 10 VOCs for OFP in Hangzhou, 2017

Scenic spot		Rural areas	
VOC species	%	VOC species	%
Ethylene	35.32	Ethylene	23.89
M/P-xylene	13.06	M/P-xylene	14.40
Toluene	10.10	Toluene	10.05
Propylene	7.86	Propylene	5.38
Ethylbenzene	4.47	N-hexane	4.87
O-xylene	3.23	O-xylene	4.83
N-butane	2.90	Ethylbenzene	3.75
N-hexane	2.82	3-Methylpentane	3.33
Propane	2.57	Isopentane	2.08
Isobutane	2.49	Isobutane	1.95
Total	84.80		74.53

The temperatures of the scenic spot were 1.12 °C, 1.34 °C, 1.15 °C and 1.48 °C higher than those of the rural area in spring, summer, autumn and winter, respectively, and the diurnal UHI was more intense than the nocturnal one.

3.2 Regional/Long-Range Transport and Local Sector Contribution of Ground-Level O_3

Hangzhou has distinct four seasons and we selected the daily average data in January, April, July and October of 2017, representing spring, summer, autumn and winter, respectively, to simulate using WRF-CMAQ.

3.2.1 Model Validation

Figure 4 indicated that the trends of simulation agreed well with the observations, as Astitha et al. (2017) highlight that WRF-CMAQ is good at predicting ozone changes. Mean fractional bias (MFB) and mean fractional error (MFE) demonstrated the simulations for all 4 months (MFB$\leqslant \pm 28\%$ and MFE$\leqslant +40\%$) were within the best atmospheric model performance criteria range proposed by Boylan and Russell (2006).Therefore, the WRF-CMAQ was to be considered accurate in simulating the ground-level O_3 throughout the year in Hangzhou. The most accurate simulation was in July followed by April, October and January. The relative poor performance in January was because the chemical mechanism (CB05) was not functioning well when the temperature is low.

3.2.2 Regional/Long-Range Transport of O_3 Estimated by WRF-CMAQ

The zero-out strategy (Cho et al. 2012; Feng et al. 2019) was applied to estimate the regional transport/long-range transport of ground-level O_3 over Hangzhou. The outcome showed that regional/long-range transport accounted for 17.4%, 14.5%, 19.7% and 15.4% of the ground-level O_3 in January, April, July and October of 2017, respectively. Northerly wind prevailed in winter and autumn while southwesterly wind prevailed in spring and summer, as Fig. 5 indicates. Hence, the regional/long-range ground-level O_3 transport showed the pattern of southwest-to-northeast in spring and summer and north-to-south in autumn and winter, which was primarily influenced by the East Asian monsoon climate (Li et al. 2016a). Figure 6 illustrated the monthly average of O_3 over YRD. Hangzhou locates at the center of the dotted cross.

3.2.3 Local Hangzhou Sectors Contribution

The local Hangzhou pollution emission sources were divided into four separately sectors: agriculture (including crops-

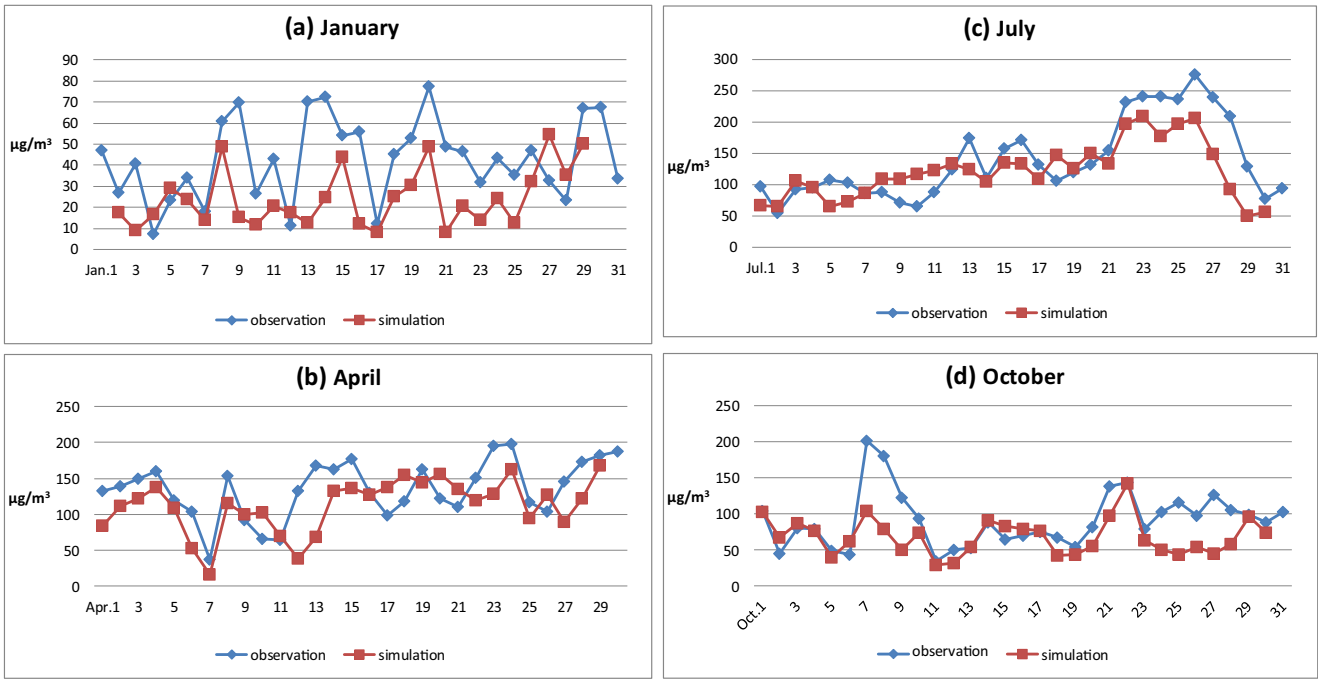

Fig. 4 Observed and simulated O_3-24h in 2017: **a** January; **b** April; **c** July; **d** October

Fig. 5 Wind rose of Hangzhou in 2017

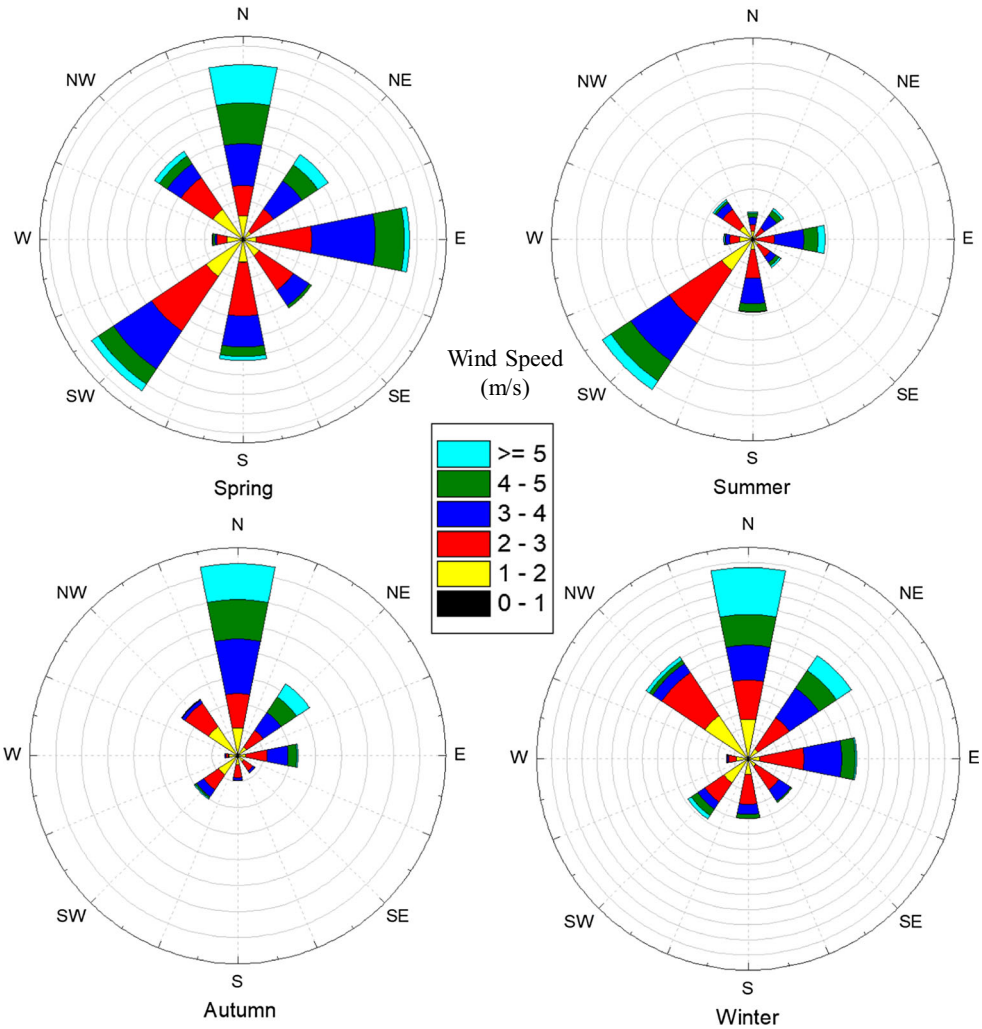

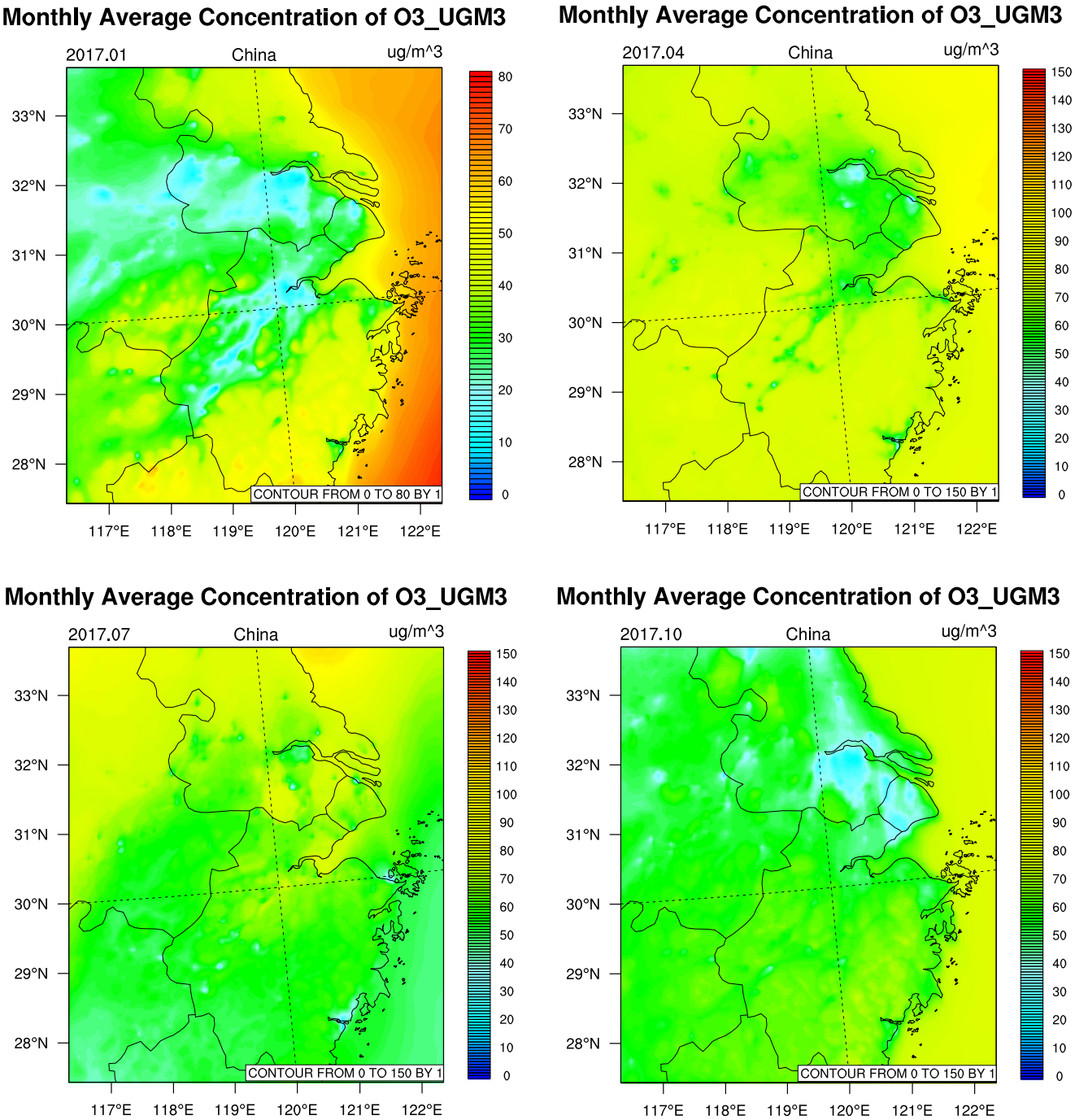

Fig. 6 Monthly average O_3-24h upon YRD, 2017

burning), residence, industry and traffic. The zero-out strategy was used to calculate the individual sector contribution for O_3.

The local sectors contributions, given in Table 3, indicated that industry was the primary contributor of O_3. The reason that traffic produces less O_3 than industry and residence was local traffic donated about 82% of annual average NO_2 (Feng et al. 2019), as high NO_2 inhibited the O_3 in VOC-limited regime. The vertical O_3 transport from stratosphere to the troposphere (Liu et al. 2010) needs to be further investigated.

Table 3 Local sector contribution to local produced O_3 at the scenic spot

	Agriculture	Residence	Industry	Traffic
January	2.2%	32.6%	60.5%	4.7%
April	3.1%	37.5%	55.6%	3.8%
July	2.3%	29.7%	65.0%	3.0%
October	2.9%	37.7%	55.8%	3.6%
Average	2.6%	34.4%	59.2%	3.8%

4 Conclusions

A detailed ground-level O_3 control strategy is proposed using observed data and the atmospheric model WRF-CMAQ. All the analysis made in this paper is either from observation or model simulation.

We revealed the following highlights:

(1) Hangzhou belongs to VOC-limited regime. Reduction of NOx or escalation of VOCs results in increase of tropospheric O_3 and vice versa.
(2) The Western North Pacific Subtropical High was one of the most important influential factors for shaping O_3. The direct solar radiation time had less impact on O_3 change when it's more than 4 h in a day.
(3) The ground-level ozone index formula was able to characterize the monthly and daily ground-level O_3-8h level in Hangzhou throughout the year and indicated the ground-level O_3 was positively correlated to temperature, VOCs and direct solar radiation time while negatively correlated to relative humidity, precipitation, wind speed and NO_2.
(4) Ethylene, m/p-xylene, toluene and propylene were the major contributors to O_3.
(5) WRF-CMAQ was within the best atmospheric model performance criteria range in simulating O_3. The long-range/regional transport accounted for 15.4% and 17.4% of O_3 in autumn and winter, respectively, showing a north-to-south transport pattern while 14.5% and 19.7% of O_3 in spring and summer, respectively, showing a southwest-to-northeast transport pattern.
(6) Annual local O_3 contribution for industry was 59.2% in the downtown Hangzhou, followed by residence, traffic and agriculture in 2017.

Therefore, we have the following suggestions to mitigate the ground-level ozone pollution. Due to the NO_2 reduction plan by 2020, controlling VOCs, especially alkenes and aromatics, is the most effective way to lower O_3. Artificial precipitation is a possible way to decrease ground-level O_3, because it can block the solar radiation, lower temperature and add humidity. Afforestation should be implemented to abate UHI. Shutdown local industry and the VOCs emitted sources outside Hangzhou in the upwind direction during important events.

Acknowledgments This work is financially supported by the National Natural Science Foundation of China (Nos. 51390493 and 51476144).

Compliance with Ethical Standards

Conflict of Interest The authors declare no conflicts of interest.

References

Alvim, D., Gatti, L., Corrêa, S., Chiquetto, J., Santos, G., Rossatti, C., Pretto, P., Rozante, J., Figueroa, S., Pendharkar, J., Nobre, P.: Determining VOCs reactivity for ozone forming potential in the megacity of São Paulo. Aerosol Air Qual. Res. **18**(9), 2460–2474 (2017). https://doi.org/10.4209/aaqr.2017.10.0361

Astitha, M., Luo, H., Rao, T., Hogrefe, C., Mathur, R., Kumar, N.: Dynamic evaluation of two decades of WRF-CMAQ ozone simulations over the contiguous United States. Atmos. Environ. **164**, 102–116 (2017). https://doi.org/10.1016/j.atmosenv.2017.05.020

Barnes, B., Cannizzaro, J., English, D., Hu, C.: Validation of VIIRS and MODIS reflectance data in coastal and oceanic waters: An assessment of methods. Remote Sens. Environ. **220**, 110–123 (2019). https://doi.org/10.1016/j.rse.2018.10.034

Boylan, J.W., Russell, A.G.: PM and light extinction model performance metrics, goals, and criteria for three-dimensional air quality models. Atmos. Environ. **40**(26), 4946–4959 (2006). https://doi.org/10.1016/j.atmosenv.2005.09.087

Breedt, H., Craig, K., Jothiprakasam, V.: Monin-Obukhov similarity theory and its application to wind flow modelling over complex terrain. J. Wind Eng. Ind. Aerodyn. **182**, 308–321 (2018). https://doi.org/10.1016/j.jweia.2018.09.026

Carter, W.: Development of the SAPRC-07 chemical mechanism. Atmos. Environ. **44**(40), 5324–5335 (2010). https://doi.org/10.1016/j.atmosenv.2010.01.026

Carter, W., Seinfeld, J.: Winter ozone formation and VOC incremental reactivities in the Upper Green River Basin of Wyoming. Atmos. Environ. **50**, 255–266 (2012). https://doi.org/10.1016/j.atmosenv.2011.12.025

Chan, K., Yao, X.: Air pollution in mega cities in China. Atmos. Environ. **42**(1), 1–42 (2008). https://doi.org/10.1016/j.atmosenv.2007.09.003

Chan, K., Wang, S., Liu, C., Zhou, B., Wenig, M., Saiz-Lopez, A.: On the summertime air quality and related photochemical processes in the megacity Shanghai, China. Sci. Total Environ. **580**, 974–983 (2017). https://doi.org/10.1016/j.scitotenv.2016.12.052

Chen, Y., Zhu, Z., Luo, L., Zhang, J.: Severe haze in Hangzhou in winter 2013/14 and associated meteorological anomalies. Dyn. Atmos. Oceans. **81**, 73–83 (2018). https://doi.org/10.1016/j.dynatmoce.2018.01.002

Cho, S., Morris, R., McEachern, P., Shah, T., Johnson, J., Nopmongcol, U.: Emission sources sensitivity study for ground-level ozone and $PM_{2.5}$ due to oil sands development using air quality modeling system: part II- source apportionment modeling. Atmos. Environ. **55**, 542–556 (2012). https://doi.org/10.1016/j.atmosenv.2012.02.025

Dong, H., Cao, S., Takemi, T., Ge, Y.: WRF simulation of surface wind in high latitudes. J. Wind Eng. Ind. Aerodyn. **179**, 287–296 (2018). https://doi.org/10.1016/j.jweia.2018.06.009

Feng, R., Wang, Q., Huang, C., Liang, J., Luo, K., Fan, J., Zheng, H.: Ethylene, xylene, toluene and hexane are major contributors of atmospheric ozone in Hangzhou, China, prior to the 2022 Asian games. Environ. Chem. Lett. (2018). https://doi.org/10.1007/s10311-018-00846-w

Feng, R., Wang, Q., Huang, C., Liang, J., Luo, K., Fan, J., Cen, K.: Investigation on air pollution control strategy in Hangzhou for post-G20/pre-Asian-games period (2018–2020). Atmos. Pollut. Res. **10**(1), 197–208 (2019). https://doi.org/10.1016/j.apr.2018.07.006

Fountoukis, C., Martín-Pomares, L., Perez-Astudillo, D., Bachour, D., Gladich, I.: Simulating global horizontal irradiance in the Arabian Peninsula: sensitivity to explicit treatment of aerosols. Sol. Energy. **163**, 347–355 (2018). https://doi.org/10.1016/j.solener.2018.02.001

Fu, Q., Mo, Z., Lyu, D., Zhang, L., Qin, Z., Tang, Q., Yin, H., Xu, P., Wu, L., Lou, X., Chen, Z., Yao, K.: Air pollution and outpatient visits for conjunctivitis: a case-crossover study in Hangzhou, China. Environ.

Pollut. **231**(2), 1344–1350 (2017). https://doi.org/10.1016/j.envpol.2017.08.109

Ganeshan, M., Murtugudde, R., Imhoff, M.: A multi-city analysis of the UHI-influence on warm season rainfall. Urban Climate. **6**, 1–23 (2013). https://doi.org/10.1016/j.uclim.2013.09.004

Gao, J., Zhu, B., Xiao, H., Kang, H., Hou, X., Shao, P.: A case study of surface ozone source apportionment during a high concentration episode, under frequent shifting wind conditions over the Yangtze River Delta, China. Sci. Total Environ. **544**, 853–863 (2016). https://doi.org/10.1016/j.scitotenv.2015.12.039

Gao, W., Tie, X., Xu, J., Huang, R., Mao, X., Zhou, G., Chang, L.: Long-term trend of O_3 in a mega City (Shanghai), China: characteristics, causes, and interactions with precursors. Sci. Total Environ. **603-604**, 425–433 (2017). https://doi.org/10.1016/j.scitotenv.2017.06.099

Geng, F., Tie, X., Xu, J., Zhou, G., Peng, L., Gao, W., Tang, X., Zhao, C.: Characterizations of ozone, NOx, and VOCs measured in Shanghai, China. 42 (29). Atmos. Environ. **42**(29), 6873–6883 (2008). https://doi.org/10.1016/j.atmosenv.2008.05.045

Geng, F., Qiang, Z., Tie, X., Huang, M., Ma, X., Deng, Z., Quan, J., Zhao, C.: Aircraft measurements of O3, NOx, CO, VOCs, and SO2 in the Yangtze River Delta region. Atmos. Environ. **43**, 584–593 (2009). https://doi.org/10.1016/j.atmosenv.2008.10.021

Geng, F., Tie, X., Guenther, A., Li, G., Cao, J., Harley, P.: Effect of isoprene emissions from major forests on ozone formation in the city of Shanghai, China. Atmos. Chem. Phys. **11**, 10449–10459 (2011). https://doi.org/10.5194/acp-11-10449-2011

He, X., Pang, S., Ma, J., Zhang, Y.: Influence of relative humidity on heterogeneous reactions of O3 and O3/SO2 with soot particles: potential for environmental and health effects. Atmos. Environ. **165**, 198–206 (2017). https://doi.org/10.1016/j.atmosenv.2017.06.049

Hou, X., Zhu, B., Fei, D., Wang, D.: The impacts of summer monsoons on the ozone budget of the atmospheric boundary layer of the Asia-Pacific region. Sci. Total Environ. **502**, 641–649 (2015). https://doi.org/10.1016/j.scitotenv.2014.09.075

Hua, Y., Xie, R., Su, Y.: Fiscal spending and air pollution in Chinese cities: identifying composition and technique effects. China Econ. Rev. **47**, 156–169 (2018). https://doi.org/10.1016/j.chieco.2017.09.007

Ito, T., Ogino, K., Nagaoka, K., Takemoto, K.: Relationship of particulate matter and ozone with 3-nitrotyrosine in the atmosphere. Environ. Pollut. **236**, 948–952 (2018). https://doi.org/10.1016/j.envpol.2017.10.069

Kishné, A., Yiman, Y., Morgan, C., Dornblaser, B.: Evaluation and improvement of the default soil hydraulic parameters for the Noah land surface model. Geoderma. **285**, 247–259 (2017). https://doi.org/10.1016/j.geoderma.2016.09.022

Kumar, M., Tsujimura, T., Suzuki, Y.: NOx model development and validation with diesel and hydrogen/diesel dual-fuel system on diesel engine. Energy. **145**, 495–506 (2018). https://doi.org/10.1016/j.energy.2017.12.148

Li, J., Yang, W., Wang, Z., Chen, H., Hu, B., Li, J., Sun, Y., Fu, P., Zhang, Y.: Modeling study of surface ozone source-receptor relationships in East Asia. Atmos. Res. **167**, 77–88 (2016a). https://doi.org/10.1016/j.atmosres.2015.07.010

Li, M., Song, Y., Mao, Z., Liu, M., Huang, X.: Impacts of thermal circulations induced by urbanization on ozone formation in the Pearl River Delta region, China. Atmos. Environ. **127**, 382–392 (2016b). https://doi.org/10.1016/j.atmosenv.2015.10.075

Li, K., Chen, L., Ying, F., White, S., Jang, C., Wu, X., Gao, X., Hong, S., Shen, J., Azzi, M., Cen, K.: Meteorological and chemical impacts on ozone formation: a case study in Hangzhou, China. Atmos. Res. **196**, 40–52 (2017). https://doi.org/10.1016/j.atmosres.2017.06.003

Li, K., Hong, L., White, S., Zheng, X., Lv, B., Lin, C., Bao, Z., Wu, X., Gao, X., Ying, F., Shen, J., Azzi, M., Cen, K.: Chemical characteristics and sources of PM1 during the 2016 summer in Hangzhou. Environ. Pollut. **232**, 42–54 (2018a). https://doi.org/10.1016/j.envpol.2017.09.016

Li, S., Wang, T., Huang, X., Pu, X., Li, M., Chen, P., Yang, X., Wang, M.: Impact of east Asian summer monsoon on surface ozone pattern in China. J. Geophys. Res.-Atmos. **123**(2), 1401–1411 (2018b). https://doi.org/10.1002/2017JD027190

Li, G., Zhang, X., Mirzaei, P., Zhang, J., Zhao, Z.: Urban heat island effect of a typical valley city in China: responds to the global warming and rapid urbanization. Sustain. Cities Soc. **38**, 736–745 (2018c). https://doi.org/10.1016/j.scs.2018.01.033

Liao, Z., Gao, M., Sun, J., Fan, S.: The impact of synoptic circulation on air quality and pollution-related human health in the Yangtze River Delta region. Sci. Total Environ. **607-608**, 838–846 (2016). https://doi.org/10.1016/j.scitotenv.2017.07.031

Liu, X., Zhang, Y., Xing, J., Zhang, Q., Wang, K., Streets, D., Jang, C., Wang, W., Hao, J.: Understanding of regional air pollution over China using CMAQ, part II: process analysis and sensitivity of ozone and particulate matter to precursor emissions. Atmos. Environ. **44**(30), 3719–3727 (2010). https://doi.org/10.1016/j.atmosenv.2010.03.036

Liu, H., Liu, S., Xue, B., Lv, Z., Meng, Z., Yang, X., Xue, T., Yu, Q., He, K.: Ground-level ozone pollution and its health impacts in China. Atmos. Environ. **173**, 223–230 (2018a). https://doi.org/10.1016/j.atmosenv.2017.11.014

Liu, Y., Li, L., An, J., Huang, L., Yan, R., Huang, C., Wang, H., Wang, Q., Wang, M., Zhang, W.: Estimation of biogenic VOCS emissions and its impact on ozone formation over the Yangtze River Delta region, China. Atmos. Environ. **186**, 113–128 (2018b). https://doi.org/10.1016/j.atmosenv.2018.05.027

Marais, E., Jacob, D., Wecht, K., Lerot, C., Zhang, L., Yu, K., Kurosu, T., Chance, K., Sauvage, B.: Anthropogenic emissions in Nigeria and implications for atmospheric ozone pollution: a view from space. Atmos. Environ. **99**, 32–40 (2014). https://doi.org/10.1016/j.atmosenv.2014.09.055

Mohr, K., Tao, W., Chern, J., Kumar, S., Peters-Lidard, C.: The NASA-Goddard multi-scale modeling framework–land information system: global land/atmosphere interaction with resolved convection. Environ. Model Softw. **39**, 103–115 (2013). https://doi.org/10.1016/j.envsoft.2012.02.023

Oyola, M., Schneider, A., Campbell, J., Joseph, E.: Meteorological influences on tropospheric ozone over suburban Washington, DC. Aerosol Air Qual. Res. **18**(5), 1168–1182 (2017). https://doi.org/10.4209/aaqr.2017.12.0574

Qian, Z.: Hangzhou. In: City Profile: Hangzhou. Cities, vol. 48, pp. 42–54 (2015). https://doi.org/10.1016/j.cities.2015.06.004

Song, C., Wu, L., Xie, Y., He, J., Chen, X., Wang, T., Lin, Y., Jin, T., Wang, A., Liu, Y., Dai, Q., Liu, B., Wang, Y., Mao, H.: Air pollution in China: status and spatiotemporal variations. Environ. Pollut. **227**, 334–347 (2017). https://doi.org/10.1016/j.envpol.2017.04.075

Tai, A., Martin, A.: Impacts of ozone air pollution and temperature extremes on crop yields: spatial variability, adaptation and implications for future food security. Atmos. Environ. **169**, 11–21 (2016). https://doi.org/10.1016/j.atmosenv.2017.09.002

Tambo, E., Wang, D., Zhou, X.: Tackling air pollution and extreme climate changes in China: implementing the Paris climate change agreement. Environ. Int. **95**, 152–156 (2016). https://doi.org/10.1016/j.envint.2016.04.010

Tan, Z., Lu, K., Jiang, M., Su, R., Dong, H., Zeng, L., Xie, S., Tan, Q., Zhang, Y.: Exploring ozone pollution in Chengdu, southwestern China: a case study from radical chemistry to O3-VOC-NOx sensitivity. Sci. Total Environ. **636**, 775–786 (2018). https://doi.org/10.1016/j.scitotenv.2018.04.286

Telesnicki, M., Martínez-Ghersa, M., Ghersa, C.: Plant oxidative status under ozone pollution as predictor for aphid population growth: the case of Metopolophium dirhodum (Hemiptera: Aphididae) in Triticum aestivum (Poales: Poaceae). Biochem. Syst. Ecol. **77**, 51–56 (2018). https://doi.org/10.1016/j.bse.2018.02.004

Tie, X., Geng, F., Guenther, A., Cao, J., Greenburg, J., Zhang, R., Apel, E., Li, G., Weinheimer, A., Chen, J., Cai, C.: Megacity impacts on regional ozone formation: observations and WRF-Chem modeling for the MIRAGE-Shanghai field campaign. Atmos. Chem. Phys. **13**, 5655–5669 (2013). https://doi.org/10.5194/acp-13-5655-2013

Wang, T., Wei, X., Ding, A.: Increasing surface ozone concentrations in the background-level atmosphere of Southern China, 1994–2007. Atmos. Chem. Phys. **9**(16), 6217–6227 (2009)

Wang, P., Schade, G., Estes, M., Ying, Q.: Improved MEGAN predictions of biogenic isoprene in the contiguous United States. Atmos. Environ. **148**, 337–351 (2017). https://doi.org/10.1016/j.atmosenv.2016.11.006

Wang, Y., Du, H., Xu, Y., Lu, D., Wang, X., Guo, Z.: Temporal and spatial variation relationship and influence factors on surface urban heat island and ozone pollution in the Yangtze River Delta, China. Sci. Total Environ. **631-632**, 921–933 (2018a). https://doi.org/10.1016/j.scitotenv.2018.03.050

Wang, Q., Li, S., Dong, M., Li, W., Gao, X., Ye, R., Zhang, D.: VOCs emission characteristics and priority control analysis based on VOCs emission inventories and ozone formation potentials in Zhoushan. Atmos. Environ. **182**, 234–241 (2018b). https://doi.org/10.1016/j.atmosenv.2018.03.034

Wie, J., Moon, B.: Impact of the Western North Pacific subtropical high on summer surface ozone in the Korean Peninsula. Atmos. Pollut. Res. **9**(4), 655–661 (2018). https://doi.org/10.1016/j.apr.2017.12.012

Wu, W.: City profile: Shanghai. Cities. **16**(3), 207–216 (1999). https://doi.org/10.1016/S0264-2751(98)00047-X

Wu, X., Chen, S., Guo, J., Gao, G.: Effect of air pollution on the stock yield of heavy pollution enterprises in China's key control cities. J. Clean. Prod. **170**, 399–406 (2018). https://doi.org/10.1016/j.jclepro.2017.09.154

Xiao, H., Sun, J., Bian, X., Dai, Z.: GPU acceleration of the WSM6 cloud microphysics scheme in GRAPES model. Comput. Geosci. **59**, 156–162 (2013). https://doi.org/10.1016/j.cageo.2013.06.016

Xu, Z., Huang, X., Nie, W., Chi, X., Xu, Z., Zheng, L., Sun, P., Ding, A.: Influence of synoptic condition and holiday effects on VOCs and ozone production in the Yangtze River Delta region, China. Atmos. Environ. **168**, 112–124 (2017). https://doi.org/10.1016/j.atmosenv.2017.08.035

Zepka, G., Pinto, O., Saraiva, A.: Lightning forecasting in southeastern Brazil using the WRF model. Atmos. Res. **135-136**, 344–362 (2014). https://doi.org/10.1016/j.atmosres.2013.01.008

Zhang, W., Wang, G., Liu, X., Feng, Z.: Effects of elevated O3 exposure on seed yield, N concentration and photosynthesis of nine soybean cultivars (Glycine max (L.) Merr.) in Northeast China. Plant Sci. **226**, 172–181 (2014). https://doi.org/10.1016/j.plantsci.2014.04.020

Zhang, Y., Qu, S., Zhao, J., Zhu, G., Zhang, Y., Lu, X., Sabel, C., Wang, H.: Quantifying regional consumption-based health impacts attributable to ambient air pollution in China. Environ. Int. **112**, 100–106 (2018). https://doi.org/10.1016/j.envint.2017.12.021

Zhao, Z., Wang, Y.: Influence of the West Pacific subtropical high on surface ozone daily variability in summertime over eastern China. Atmos. Environ. **170**, 197–204 (2017). https://doi.org/10.1016/j.atmosenv.2017.09.024

Zhao, Y., Xia, Y., Zhou, Y.: Assessment of a high-resolution NOX emission inventory using satellite observations: a case study of southern Jiangsu, China. Atmos. Environ. **190**, 135–145 (2018). https://doi.org/10.1016/j.atmosenv.2018.07.029

Zouzelka, R., Rathousky, J.: Photocatalytic abatement of NOx pollutants in the air using commercial functional coating with porous morphology. Appl. Catal. B Environ. **217**, 466–476 (2017). https://doi.org/10.1016/j.apcatb.2017.06.009